

---

## Using self organizing maps to analyze larval fish assemblage vertical dynamics through environmental-ontogenetic gradients

Álvarez I. <sup>1,\*</sup>, Font Munoz Joan Salvador <sup>1,3</sup>, Hernández-Carrasco I. <sup>1</sup>, Díaz-Gil C. <sup>1,2</sup>, Salgado-Hernanz P.M. <sup>1</sup>, Catalán I.A. <sup>1</sup>

<sup>1</sup> IMEDEA (UIB-CSIC). Miquel Marqués 21, 07190, Esporles, Spain

<sup>2</sup> Laboratori d' Investigacions Marines i Aqüicultura, LIMIA (Balearic Government), Port d'Andratx, Illes Balears, Spain

<sup>3</sup> IFREMER, French Institute for Sea Research, DYNECO PELAGOS, 29280, Plouzané, France

\* Corresponding author : I. Alvarez, email address : [itziar@imedea.uib-csic.es](mailto:itziar@imedea.uib-csic.es)

---

### Abstract :

We analyzed the influence of the stratification process in the vertical distribution of larval fish in a microtidal coastal Mediterranean zone. By applying a Self Organizing Maps (SOM) technique, we could analyze a complex dataset accounting for non-linear processes. The analysis integrated multivariate data on larval fish and environmental parameters in two depth strata through two-time components (nictimeral and fortnightly through the main spawning seasons), and considered size-based information. Although causal relationships cannot be constructed, the use of SOM analyses enabled the description of the whole system evolution overcoming the constraints of linear approaches in complex multivariate datasets with multiple dependencies in the data. We contend that this approach can help to unveil the intricate patterns of settlement/recruitment of young fish, which is often hampered by the rigidity of some formal statistical approaches.

### Highlights

► Larval fish assemblages analysis with Self Organizing Maps allows overcoming linear constraints. ► Self Organizing Maps analysis allowed the description of the whole coastal multispecific system. ► Self Organizing Maps also allowed identifying ontogenetic differences in vertical positions. ► Differences in larval fish vertical strategies before & after the establishment of stratification.

**Keywords :** Keywords: larval fish assemblages, self-organizing maps, neural networks, seasonal thermocline, vertical distribution

## 1. Introduction

29 The persistence and resilience of fish populations depend on their adaptation success at  
30 multiple scales through space and development. Bottlenecks in fish populations are  
31 often related to variability in the survival of larvae and juveniles (Houde, 2008; Nash  
32 and Geffen, 2012) and the study of their ecological adaptations has been paramount in  
33 marine ecology and fisheries science since Hjort (1926, 1914). Juvenile and adult stages  
34 of fish mainly inhabit a world dominated by inertial forces. Under those conditions, they  
35 can control their position at the horizontal scale and have more options to respond to  
36 environmental stressors. On the contrary, eggs and early larval stages inhabit a world of  
37 frictional forces, and their low (and variable) accumulated survival depends on a  
38 combination of parental adaptations to spawning (Cianelli et al., 2015) and larval  
39 adaptations to an environment over which they have more limited control (Houde and  
40 Schekter, 1980). Due to the importance of larval fish distribution and vertical  
41 positioning for recruitment (e.g., Sinclair and Iles, 1985), much research has been  
42 devoted to the analysis of larval fish movement at the vertical dimension and, at more  
43 advanced stages, at the horizontal scale (reviewed in Kingsford et al., 2002; Leis, 2006;  
44 Montgomery et al., 2001). Larval fish have a species-specific and ontogenetic-  
45 dependent capacity to conduct vertical migrations, which probably responds to trade-  
46 offs that maximize survivorship (Vikebø et al., 2005). Vertical migrations have been  
47 documented both at coastal/estuarine systems and over deep water columns. These  
48 migrations are interpreted as responses to food distribution and light, tides,  
49 stratification, predator abundance, or turbulence (see cited reviews). Studies on vertical  
50 movements usually concentrate on one or a few species and typically analyze their  
51 findings into one or a few stages or size classes. The temporal analysis of vertical  
52 patterns of multiple species and development at a high resolution is seldom conducted  
53 (but see Rodriguez et al., 2011). In addition, the usual approach with multivariate  
54 statistical methods that tend to extract only linear dependencies (or non-linear, limited  
55 to single species), limits our ability to understand how assemblages respond to complex  
56 environments.

57 One of the key controllers of larval fish dynamics at the vertical scale is stratification  
58 (Ropke, 1993; Smith et al., 1999). Thermocline formation during the stratification  
59 period acts as a physical barrier to vertical injection of subsurface nutrients to the upper  
60 layer, reducing energy inputs and generating vertical segregation of resources (Mann  
61 and Lazier, 1991). Therefore, it affects prey fields and causes physiological adaptive  
62 effects on growth, respiration, mortality and nutrient recycling (Arvola et al., 2017;

63 Nøttestad et al., 2016). In shallow coastal environments, surface water reaches high  
64 temperatures in summer, intensifying the segregation of resources and affecting thermal  
65 tolerances of some organisms, including fish larvae (Bensoussan et al., 2010).

66 The vertical distribution of fish larvae in these shallow systems may influence dispersal  
67 (Paris and Cowen, 2004; Sponaugle et al., 2002). This is the case in microtidal areas  
68 where, for example, larval retention near reefs is favoured close to the bottom layers due  
69 to the weaker flow conditions (Leis, 1986).

70 In the last decades, increased stratification of coastal waters in temperate areas, such as  
71 the Mediterranean, has been documented (e.g., Coma et al., 2009). The knowledge of  
72 the mechanisms through which fish larvae manage to inhabit stratified waters and how  
73 juveniles find the way to recruit to the adult's habitat gains interest. In the  
74 Mediterranean, the location of fish spawning is determined by the structure of the  
75 bathymetry, types of sea bottoms, diversity of adult fish habitats, and mechanisms  
76 conditioning the primary production of the region. In contrast, the physical processes  
77 determine the final distribution patterns of fish eggs and larvae (e.g., shelf-slope density  
78 front and associated current, continental water inflows, winter mixing, stratification of  
79 the water column) (Sabatés et al., 2007). Whereas some understanding exists on vertical  
80 movements of key species in open waters (e.g., Olivar et al., 2018, 2014; Olivar and  
81 Sabatés, 1997; Sabatés, 2004), little is known about the temporal-spatial ecology at the  
82 vertical scale within larval assemblages (Vargas-Yáñez and Sabatés, 2007). We contend  
83 that monitoring many species of larval fish at the vertical scale and their development  
84 during the advent of critical physical processes in coastal systems, can fill a gap in the  
85 knowledge on the relevant mechanisms influencing coastal fish populations.

86 We examined the relationship between the environmental variables during the  
87 thermocline formation and the distribution of fish larvae in the water column regarding  
88 stratification and larval ontogenetic changes in size. The complexity of the involved  
89 processes in larval fish dynamics requires analytical methods capable of including the  
90 non-linearity of the data such as Self Organising Maps (SOM) (Kohonen, 1982). This  
91 technique has been used in several disciplines, including climate and meteorology  
92 (Kolczynski and Hacker, 2014), physical and biological oceanography (Basterretxea et  
93 al., 2018; Hernández-Carrasco et al., 2018; Hernández-Carrasco and Orfila, 2018; Liu et  
94 al., 2006), genetics (Sharon et al., 2013) and even aspects of larval fish ecology (Russo  
95 et al., 2014). In our case, we used SOM to elucidate patterns in complex larvae  
96 assemblages. SOM is essentially used as a dimension reduction technique, and provides

97 advantages as compared to other widely used statistical techniques such as PCA, K-  
98 means, or other multivariate analysis (e.g., NMDS, CCA, or RDA) for several reasons:  
99 i) it allows an appropriate analysis of high dimensional data, such as the high-  
100 throughput results of the analysis of the samples; ii) it can identify and extract the  
101 underlying non-linear data structures, i.e., using step-like or Gaussian functions for the  
102 neighborhood relationship; iii) it is an efficient method for feature extraction and  
103 afterward classification, providing patterns that explain the overall behavior of the  
104 system and iv) since SOM preserves topology, patterns are ordered in the neural  
105 network according to their similitude, which finally can be easily interpreted by visual  
106 inspection (Liu et al., 2006; Mörchen and Ultsch, 2005).

107 In this work, physical and biological variables such as temperature, current speed, wave  
108 height, phytoplankton, micro, and mesozooplankton biomass, were vertically sampled  
109 through the water column and through time, so the distribution of early stages of fish in  
110 relation to stratification characteristics could be determined. We hypothesized that using  
111 SOM on this complex system we could reveal if i) the vertical distribution of (some)  
112 larval fish species changes along with the multivariate environmental shift towards a  
113 stratified system including day/night variation, and ii) if the ontogenetic stage plays an  
114 essential role in the changes in larval fish vertical distribution.

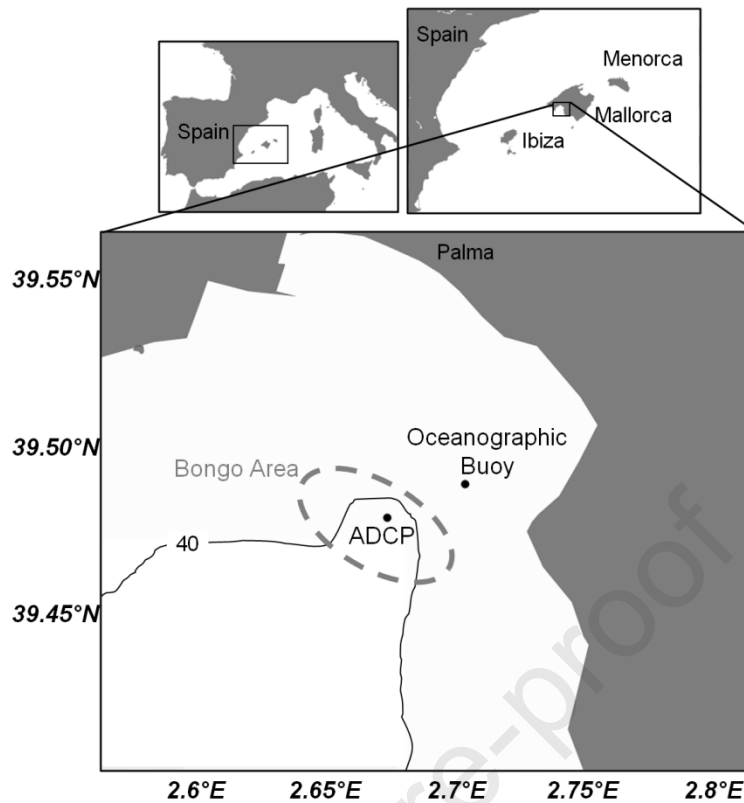
115

## 116 **2. MATERIALS AND METHODS**

117

### 118.1 *Field Sampling and Data Acquisition*

119 The field study was conducted at a single station located over a depth of 40 m (2.67°E;  
120 39.48°N) in the inner part of Palma Bay (Mallorca Island, NW Mediterranean, Fig. 1).  
121 Palma Bay was chosen due to the available abundant information on plankton dynamics  
122 in relation to physics (Alós et al., 2014; Álvarez et al., 2015b; Basterretxea et al., 2012;  
123 Font-Muñoz et al., 2018).



124

125 **Figure 1:** Map of the study area including position of the Sampling Station where the ADCP was moored  
 126 and the Oceanographic Buoy. The grey ellipse indicates the area covered by the Bongo 40 tows. The 40  
 127 m isobath is also displayed

128 Twelve surveys were fortnightly performed between April and September 2014 (from  
 129 spring to autumn). Each survey consisted of two sampling periods, conducted both at  
 130 day (around 10 GMT) and night time (just after dusk). A bottom-mounted Acoustic  
 131 Doppler Current Profiler (ADCP, 1 MHz Nortek Aquadopp) was moored at ~ 40 m  
 132 depth to characterise flow variations during all the time series in the sampling area.

133 Wave height information was obtained from an oceanographic buoy located in Palma  
 134 Bay (2.70°E; 39.49°N, Fig. 1). Data were extracted from  
 135 [http://thredds.socib.es/thredds/catalog/mooring/waves\\_recorder/buoy\\_bahiadepalma-](http://thredds.socib.es/thredds/catalog/mooring/waves_recorder/buoy_bahiadepalma-scb_wave002/L1/2014/catalog.html)  
 136 [scb\\_wave002/L1/2014/catalog.html](http://thredds.socib.es/thredds/catalog/mooring/waves_recorder/buoy_bahiadepalma-scb_wave002/L1/2014/catalog.html). The wave height (significant height) value  
 137 considered for each sampling was the mean value of the 3 hours prior to each sampling.

138 During each sampling, continuous temperature and salinity profiles were obtained with  
 139 a SBE-25 CTD and an attached handheld deployable YSI-CastAway CTD profiler. In  
 140 addition, water samples for chlorophyll analysis were collected at five depths (5, 10, 20,  
 141 30 and 40 m) using a 2.5 L Niskin bottle. Once on-board, water was filtered with GFF  
 142 filters that were immediately frozen at -20°C.

143 The instantaneous profiles of temperature from the CastAway were used to determine  
144 the thermocline depth and adapt the zooplankton sampling.

145 For micro and mesozooplankton, two consecutive hauls were conducted: one covering  
146 the whole water column (from 2 m above the sea floor to the surface) and the second  
147 above the thermocline depth. Microzooplankton was sampled with vertical hauls of a  
148 30cm diameter WP2 net fitted with a 53  $\mu\text{m}$  nylon mesh. Mesozooplankton samples  
149 were obtained with a Bongo-40 net. One side was equipped with a 335  $\mu\text{m}$  mesh net for  
150 ichthyoplankton identification and abundance estimates, and the other side was  
151 equipped with a 200  $\mu\text{m}$  mesh for the mesozooplankton biomass estimates. The Bongo-  
152 40 tows over the whole water column consisted of a double-oblique tow down to 2 m  
153 above the seafloor. The above-thermocline hauls consisted of triple-oblique tows from  
154 thermocline depth to surface. Both types of tows were conducted at a boat speed of ~2  
155 knots. The volume of water filtered was estimated by two GO 230 flowmeters mounted  
156 in the mouth of each net. Samples were preserved immediately after collection in 2%  
157 seawater borax buffered formalin.

158

#### 159 2.2 *Sample treatment*

160

161 Chlorophyll (Chl-a,  $\text{mg m}^{-3}$ ) was estimated from 24-hour acetone (90%) extracts using a  
162 Turner Designs bench fluorometer.

163 Microzooplankton samples were fractionated through 53 and 200  $\mu\text{m}$  mesh filters, and  
164 only the fraction between 53-200  $\mu\text{m}$  was retained. Dry weight from this fraction was  
165 obtained following Lovegrove (1966), and data were standardized to  $\text{mg m}^{-3}$ .

166 The 200  $\mu\text{m}$  mesh of the Bongo samples was used to determine mesozooplankton dry  
167 weight. Samples were filtered through 200 and 500  $\mu\text{m}$  meshes, and the 200-500 $\mu\text{m}$   
168 fraction retained. Dry weight was estimated and standardized as for microzooplankton.

169 Fish larvae were sorted from the 335  $\mu\text{m}$  net of the Bongo samples and identified to the  
170 lowest possible taxonomic level using a stereoscopic microscope. Larval abundance  
171 values were standardized to surface area ( $\text{ind. } 10 \text{ m}^{-2}$ ). A picture of each larva was taken  
172 with a digital camera mounted on the stereomicroscope, and total length (TL) measures  
173 were calculated with ImageJ software (Schneider et al., 2012) to the nearest 0.01mm.  
174 No correction for shrinkage was made. In order to facilitate the description of the taxa  
175 collected, class lengths were described as follows: L1 groups all larvae with sizes  
176 comprised between 1 and 2 mm; L2 groups the 2.01-3 mm larvae, and so forth until L14

177 for larvae with lengths ranging between 14.01 and 15 mm. In addition, for each taxon,  
 178 larvae were grouped into pre and postflexion groups following the available  
 179 bibliography (Table 1).

180 **Table 1.** Notochord flexion lengths from published literature sources. **FL:** Flexion length in mm.  
 181 \*Somarakis and Nikolioudakis, 2010

Family	Lower Taxa Identified	Reference Taxa	FL (mm)	Area	Reference
Ammodytidae	<i>Gymnammodytes cicereus</i>	<i>Gymnammodytes cicereus</i>	11	Balearic Sea	Alemaný, 1997 Ré and Meneses, 2009
Argentinidae	Sphyrænidae	<i>Argentina sphyræna</i> <i>Parablennius</i>	13-17	Portugal	
Blenniidae	Blenniidae	<i>tentacularis</i>	6.4	Balearic Sea	Alemaný 1997
Bothidae	<i>Arnoglossus</i> spp.	<i>Arnoglossus laterna</i>	6	Balearic Sea	Alemaný 1997
Bothidae	<i>Bothus</i> spp.	<i>Bothus podas</i>	7	Balearic Sea	Alemaný 1997
Callionymidae	Callyonimidae	Callyonimidae A <i>Trachurus</i>	4.1	Balearic Sea	Alemaný 1997
Carangidae	<i>Trachurus</i> spp.	<i>mediterraneus</i>	4.8	Balearic Sea	Alemaný 1997
Centracanthidae	<i>Spicara flexuosa</i>	<i>Spicara smarís</i>	5.5	Balearic Sea	Alemaný 1997
Centracanthidae	<i>Spicara smarís</i>	<i>Spicara smarís</i>	5.5	Balearic Sea	Alemaný 1997
Clupeidae	<i>Sardinella aurita</i>	<i>Sardinella aurita</i>	7.5-10	Atlantic Gulf of Mexico	Richards, 2006 Ditty et al., 1994 Som. and Niko. 2010*
Coryphaenidae	<i>Coryphaena hippurus</i> <i>Engraulis</i>	<i>Coryphaena hippurus</i> <i>Engraulis</i>	7.5-9		
Engraulidae	<i>encrasicolus</i>	<i>encrasicolus</i> <i>Lepadogaster</i>	10	Aegean	Tojeira et al., 2012
Gobiesocidae	Gobiesocidae	<i>lepadogaster</i>	7.1	Portugal	
Gobiidae	Gobiidae	<i>Lebetus guilleti</i> <i>Pomatoschistus</i>	3.1	Balearic Sea	Alemaný 1997
Gobiidae	Gobiidae	<i>microps</i>	3.5	Balearic Sea	Alemaný 1997
Gonostomatidae	<i>Cyclothone braueri</i>	<i>Cyclothone braueri</i>	6	Balearic Sea	Alemaný 1997
Labridae	<i>Coris julis</i>	<i>Coris julis</i>	5	Balearic Sea	Alemaný 1997
Labridae	Labridae	<i>Symphodus</i> spp. <i>Thalassoma</i>	3.1	Balearic Sea	Alemaný 1997
Labridae	<i>Thalassoma pavo</i>	<i>bifasciatum</i>	3	Atlantic	Richards 2006
Mullidae	<i>Mullus barbatus</i>	<i>Mullus barbatus</i>	3.5	Balearic Sea	Alemaný 1997
Mullidae	<i>Mullus surmuletus</i> <i>Ceratoscopelus</i>	<i>Mullus surmuletus</i> <i>Ceratoscopelus</i>	4	Balearic Sea	Alemaný 1997
Myctophidae	<i>maderensis</i>	<i>maderensis</i>	5.5	Balearic Sea	Alemaný 1997
Ophidiidae	Ophidiidae	<i>Ophidion barbatum</i> <i>Paralepis</i>	9	Balearic Sea	Alemaný 1997
Paralepididae	Paralepididae	<i>coregonoides</i>	10-15	Atlantic	Richards 2006
Pomacentridae	<i>Chromis chromis</i>	<i>Chromis chromis</i>	3.5	Balearic Sea	Alemaný 1997
Scombridae	<i>Auxis rochei</i>	<i>Auxis rochei</i>	5.4	Balearic Sea	Alemaný 1997
Scombridae	<i>Thunnus thynnus</i>	<i>Thunnus thynnus</i>	6	Atlantic	Richards 2006
Scophthalmidae	<i>Lepidorhombus boscii</i>	<i>Lepidorhombus boscii</i>	5.9	Catalan Sea	Sabatés, 1989
Scorpaenidae	<i>Scorpaena porcus</i>	<i>Scorpaena porcus</i>	3.4	Balearic Sea	Alemaný 1997
Scorpaenidae	<i>Scorpaena</i> spp.	<i>Scorpaena notata</i>	4	Balearic Sea	Alemaný 1997
Serranidae	<i>Anthias anthias</i>	<i>Anthias anthias</i>	3.3	Balearic Sea	Alemaný 1997
Serranidae	<i>Serranus hepatus</i>	<i>Serranus hepatus</i>	5.5	Balearic Sea	Alemaný 1997
Serranidae	<i>Serranus</i> spp.	<i>Serranus cabrilla</i>	4.8	Balearic Sea NW	Alemaný 1997 Ramos et al., 2010
Soleidae	Soleidae	<i>Solea senegalensis</i>	4.5	Portugal	
Sparidae	<i>Boops boops</i>	<i>Boops boops</i>	5.5	Balearic Sea	Alemaný 1997
Sparidae	<i>Diplodus</i> spp.	<i>Diplodus annularis</i>	5.2-	Catalan Sea	Sabates 1989

			5.6		
Sparidae	<i>Oblada melanura</i>	<i>Oblada melanura</i>	4.8	Catalan Sea	Sabates 1989
Sparidae	<i>Pagrus pagrus</i>	<i>Pagrus pagrus</i>	4.1	Atlantic	Richards 2006
Sparidae	Sparidae spp.	<i>Pagellus acarne</i>	5	Catalan Sea	Sabates 1989
				French	
Synodontidae	<i>Synodus saurus</i>	<i>Synodus</i>	9	polinesia	Leis et al., 2003
Trachinidae	<i>Trachinus draco</i>	<i>Trachinus draco</i>	5.1	Balearic Sea	Alemaný 1997
					McBride et al.,
Triglidae	Triglidae	<i>Prionotus</i> spp.	6	New Jersey	2002

182

183

1842.3 *Data analysis*

185 Self-Organizing Maps (SOM) were used to explore the interaction between  
 186 environmental variables and the vertical distribution of fish larvae. SOM is a non-linear  
 187 mapping implementation used to unveil underlying patterns or structures in complex  
 188 datasets, reducing the high dimensional feature space of the input data to a lower  
 189 dimensional (usually two dimensional) networks of maps called neurons. SOM is based  
 190 on unsupervised machine learning algorithms for the training of an artificial neural  
 191 network (Kohonen, 1997, 1982) that simulates the topological distribution of neuron  
 192 responses in the brain during the learning process, in particular by the relationship  
 193 between neighboring neurons.

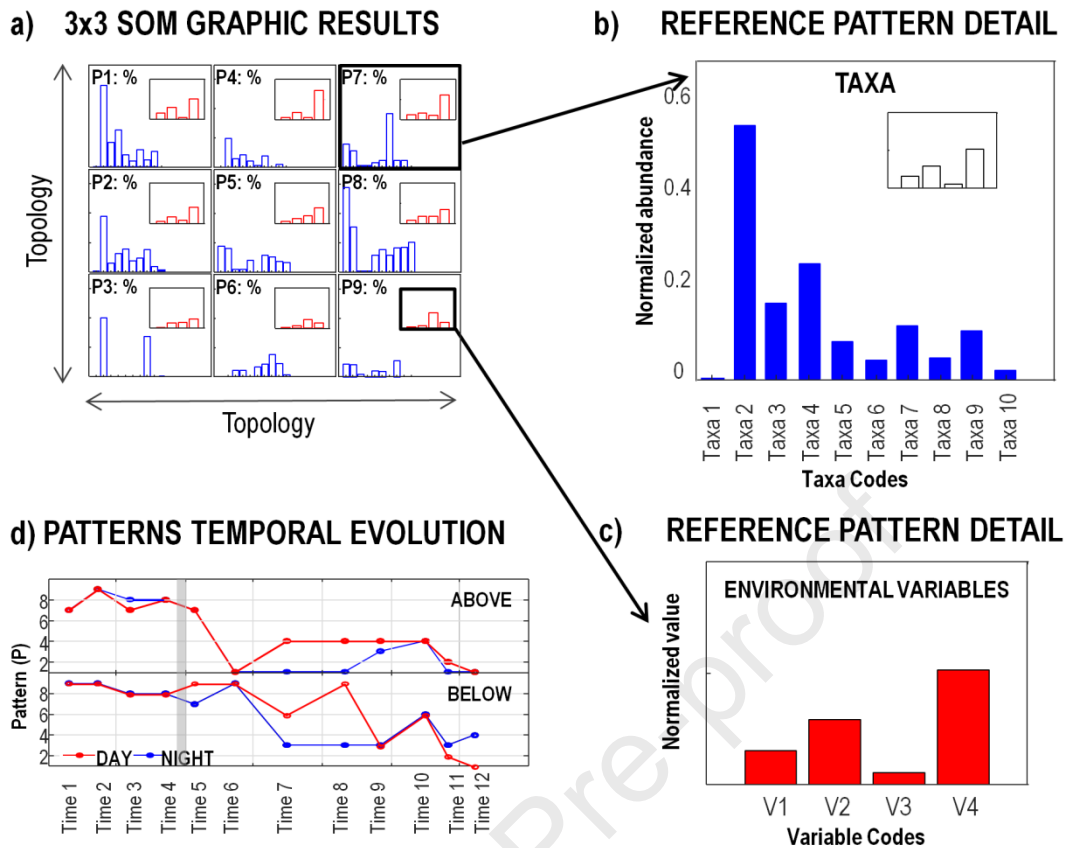
194 The learning process requires two main prerequisites. First, an input vector,  
 195 representing the data to be analyzed. In our case, the input vector was composed of  
 196 abundance taxa concatenated with each sampling's associated environmental variables  
 197 (see below a detailed description of the analyzed data matrix). Second, the parameters  
 198 that control the initialization and training processes.

199 Following Liu et al., 2006, we used an hexagonal map lattice to avoid anisotropy  
 200 artifact, and a linear combination of the first two leading Empirical Orthogonal  
 201 Functions (EOFs) modes for the initialization, although other initial configurations (e.g.,  
 202 random values) yield similar results. The training was performed using the imputation  
 203 batch training algorithm (Vatanen et al., 2015) and a Gaussian neighborhood function.  
 204 The visualization of the SOM output often forms the key interface between the  
 205 algorithm output and the user (Schreck, 2010). For clarity, a diagram of the SOM output  
 206 used in this work, and its interpretation, is presented in Fig. 2.

207 The SOM analysis consists basically of an iterative presentation of the input data to a  
 208 preselected neuronal network, which is iteratively modified. Each neuron (or unit) in the  
 209 preselected network, is represented by a weight vector with the number of components  
 210 equal to the dimension of the input sample data (abundance data and related

211 environmental data in our case). In each iteration, the neuron whose weight vector is  
212 closest (more similar) to the presented sample input data vector, called Best-Matching  
213 Unit (BMU), is transformed together with its topological neighbours towards the input  
214 sample following a specific neighbouring function. At the end of the training process,  
215 the probability density function of the input data is approximated by the SOM, and each  
216 neuron (unit) is associated with a reference pattern, with a number of components equal  
217 to the number of variables in the dataset so that it can be interpreted as a local summary  
218 or generalization of similar observations (Fig. 2a).

219 The explored matrix of environmental data includes the following variables above and  
220 below thermocline: the current speed ( $C$ ,  $\text{m s}^{-1}$ ), temperature ( $T$ ,  $^{\circ}\text{C}$ ), wave height ( $W$ ,  
221  $\text{m}$ ), micro- ( $M_i$ ,  $\text{mg m}^{-3}$ ), and mesozooplankton biomass ( $M_e$ ,  $\text{mg m}^{-3}$ ) and Chl-a ( $\text{Chl}$ ,  
222  $\text{mg m}^{-3}$ ). A second matrix was built, consisting of larval abundances, disaggregated by  
223 taxa, length (pre and post-flexion), depth stratum, day/night, and sampling day. Each  
224 variable was separately normalized in the range between [0 1]. The response of larvae to  
225 environmental variables was analyzed, coupling physical and biological patterns  
226 through SOM. A preliminary test was performed to determine the optimal number of  
227 units in the neural network. The selection of the number of neurons is not evident and  
228 depends on the complexity of the data, on the features which one wants to examine in  
229 the dataset, and also in order to minimize the quantization and topographic errors. These  
230 two errors are the most relevant and broadly quality metrics used to evaluate the  
231 performance of SOM algorithm (Vatanen et al., 2015). When using a reduced number of  
232 neurons to 4 or 6, the associated errors increased with respect to a neural network of 9  
233 neurons. On the other hand, when using 16 neurons, the quantization and topographic  
234 errors were very low, but a significant number of the patterns had 0% probability of  
235 occurrence to be represented among our data. Finally, we chose nine neurons as the best  
236 balance between associated errors and pattern representation without losing variability  
237 of the multivariate dataset (see Hernández-Carrasco and Orfila, 2018 for a more detailed  
238 analysis on the size of SOM). Finally, the potential of the technique for analyzing  
239 particularly frequent single-species with detailed larval length information (several size  
240 bins) was assessed in a similar way.



241

242 **Figure 2:** Diagram of the SOM output. a) Nine reference patterns extracted from a 3x3 coupled  
 243 SOM analysis of taxa abundances (blue) and associated environmental parameters (red). Pn:  
 244 probability of finding that particular pattern n in the data. b) Detail of the reference  
 245 pattern output for the abundance data (normalized). In this pattern, Taxa 2 and 4 would be the most  
 246 abundant and Taxa 1 abundance is almost incidental. c) Detail of the reference pattern  
 247 output for the environmental data associated with a determined output pattern for abundance data.  
 248 The number of environmental variables (normalized) corresponds to the number in the input  
 249 vectors (V). d) Representation of the temporal succession of the extracted patterns. This output  
 250 allows to identify the reference patterns that better describe the data at a given sampling time  
 251 (Time n), namely position in relation to the thermocline (above/below) and moment of the day  
 252 (day/night). The shaded area has been included to help the readers to identify the onset of the  
 253 seasonal thermocline.

254

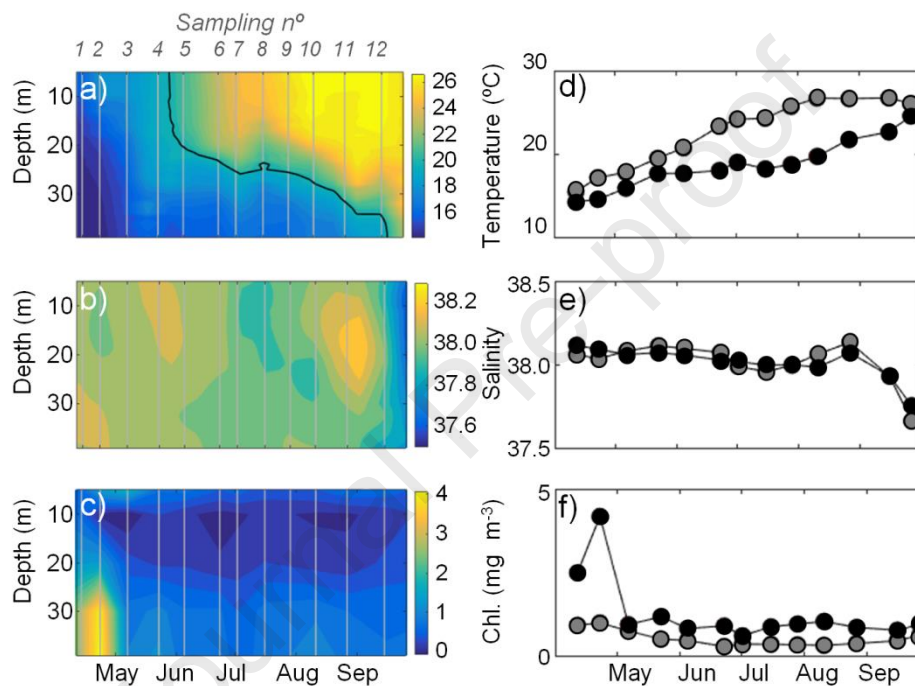
### 255 3. RESULTS

256

#### 257 3.1. Hydrographic Scenario

258 Hydrographic data shows the typical spring to summer transition in Palma Bay where  
 259 water column stratification is governed by the seasonal evolution of temperature (Fig.  
 260 3a). Since salinity was mostly uniform during the study period (Figs. 3 b, e), we  
 261 selected the 20°C isotherm as indicative of the thermocline depth. From late May to  
 262 September, progressive seasonal warming of the mixing surface layer generated a sharp

263 thermal gradient at depths of 20 to 30 m. At the end of September, the mixing surface  
 264 layer reached the bottom. Differences between average temperature above or below the  
 265 thermocline showed maxima in July-August, and almost no differences between the  
 266 initial and final times of the sampling period, confirming a correct sampling of the  
 267 stratification process (Fig. 3d). Day/night differences in temperature were not detected  
 268 and were not included as a variable in the SOM analysis. Salinity values were very  
 269 uniform throughout the season, showing typical rainfall events at the end of summer  
 270 (Fig. 3b, e).



271

272 **Figure 3:** Environmental variables. Left Column: Vertical-Temporal evolution; Numbers 1-12 indicate  
 273 the sampling number, in chronological order. Right Column: Above- (grey) and Below-Thermocline  
 274 (black) values of: Temperature (°C; a and d), Salinity (b and e) and Chlorophyll (mg m<sup>-3</sup>; c and f).

275

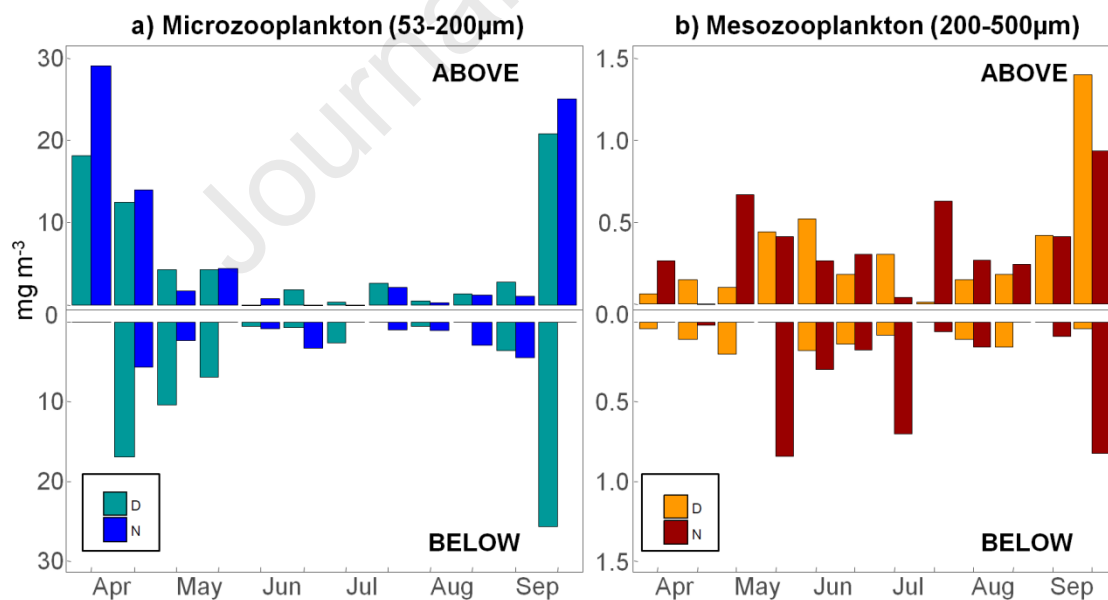
276 Surface current velocities (not shown) were consistently higher than the bottom ones  
 277 except at the end of the sampling period when velocities were almost the same. The  
 278 maximum surface current velocity (0.09 m s<sup>-1</sup>) was recorded in August, and the  
 279 minimum (0.02 m s<sup>-1</sup>) was found in April. Minimum and maximum values for the  
 280 bottom current speed (0.006 and 0.03 m s<sup>-1</sup>) were recorded in July and September,  
 281 respectively. Wave height values were consistently higher during daytime than during  
 282 night-time, with maximum differences in summer, coinciding with the breeze regime of  
 283 the area. The maximum wave height (0.75 m) occurred at the end of May.

284

## 285 3.2. Biological Scenario

286 Figure 3c shows the evolution of phytoplankton biomass, approximated from Chl-a  
 287 measurements. This evolution from high to very low values was consistent with the  
 288 seasonal variation described for the coastal waters of the Balearic Islands (e.g., Álvarez  
 289 et al., 2012). The maximum Chl-a concentration was observed during April close to the  
 290 bottom (depth >30m, Chl-a > 2.2 mg m<sup>-3</sup>). The progressive seasonal water warming  
 291 induces the development of the thermocline, and its presence and position in the water  
 292 column prevented the vertical supply of nutrients to the surface layer, limiting surface  
 293 phytoplankton biomass production during summer (< 0.1 mg m<sup>-3</sup>).

294 Microzooplankton biomass values above and below the thermocline showed the highest  
 295 values at the beginning (April) and at the end (September) of the study period (Fig. 4a).  
 296 In the absence of thermocline (at the beginning and end of the sampling period), high  
 297 microzooplankton values were observed (12.4 to ~29 mg m<sup>-3</sup>). At the beginning of  
 298 April, they were confined to the first 20 meters (both night and day). For the heavily  
 299 stratified period, June to August, values above and below the thermocline ranged  
 300 between 0.4 and 4.4 mg m<sup>-3</sup>, although below the thermocline, values were still higher  
 301 during the daytime during May (7-10.5 mg m<sup>-3</sup>).



302

303 **Figure 4:** Biotic scenario. Above- and Below-thermocline Micro and Mesozooplankton day and night  
 304 values of dry weight (biomass, mg m<sup>-3</sup>) at each sampling day. D: Day; N: Night

305 Mesozooplankton biomass values (Fig. 4b) oscillated between 0.012 and 1.703 mg m<sup>-3</sup>.  
 306 Higher values developed approximately one month later with respect to  
 307 microzooplankton. In general, daytime values were higher above the thermocline,

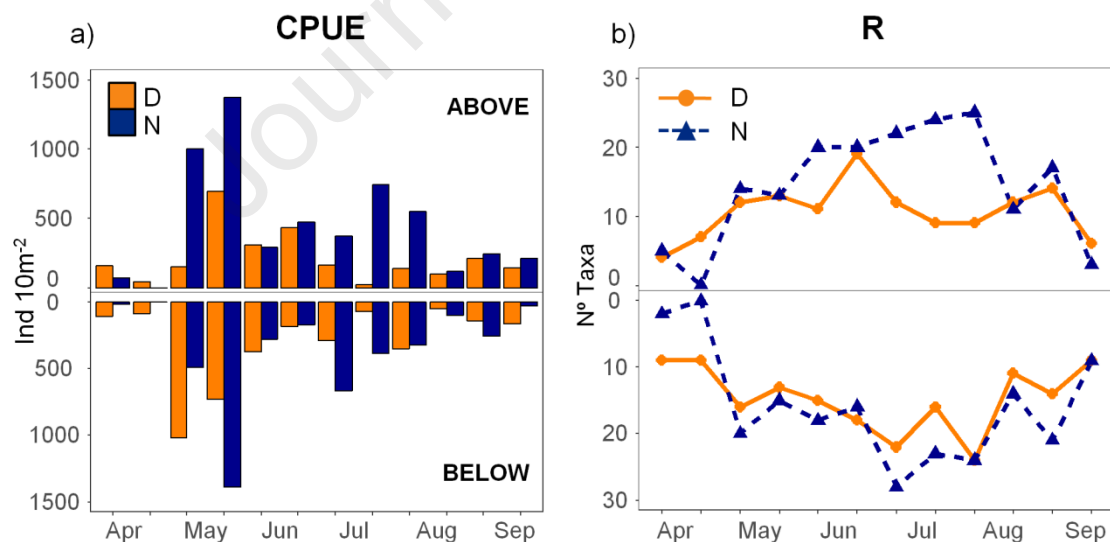
308 whereas the highest night-time values could be high both above and below the  
 309 thermocline during the stratified period. At the end of the sampling (the entire water  
 310 column was heated, see Fig. 3a), a clear difference pattern emerged, with daytime  
 311 mesozooplankton being captured in the first 20 m and spreading throughout the column  
 312 during the night (Fig. 4b).

313

### 314 3.3. Larval Fish Assemblages (LFA)

315 A total of 12284 fish larvae were found. Maximum larval fish abundances were  
 316 observed at the end of May (Fig. 5a) followed by intermediate values during the  
 317 summer months (June, July, August). In general, night abundances were higher than  
 318 during the day, and no apparent differences between above and below thermocline  
 319 larval abundances were found (Fig. 5b). The number of species (R) followed a dome-  
 320 shaped curve, with the lowest number of taxa at the beginning (overall minimum in  
 321 April in all sampling combinations) and at the end of the sampling period (Fig. 5c).

322 The dome-shaped relationship of R with time, similar to the total abundances, involved  
 323 clear dependencies of nictimeral patterns with date, i.e., high/low abundances in one  
 324 date tended to be reflected both above and below the thermocline and during day and  
 325 night.



326

327 **Figure 5:** Larval fish assemblages. Above- and Below-thermocline day and night values at each sampling  
 328 day of a) Catch-per-unit-effort (CPUE) and b) Richness (number of different taxa, R). D: Day; N: Night

329

330 The species *Spicara smaris*, *Engraulis encrasicolus* and larvae from the Gobiidae  
 331 family represented 62.07 % of the total abundance (Table 2). Some taxa were found

332 equally at day and night tows (e.g., *S. smarís*, Labridae, *Arnoglossus* spp.), whereas  
 333 some groups presented higher abundances during the night than during the day  
 334 (Gobiidae, *Sardinella aurita*, *Chromis chromis*, Table 2). *Boops boops* and *Thunnus*  
 335 *thynnus* followed the opposite pattern with higher daytime abundances. Few groups  
 336 were only found at night hauls (e.g., *Thalassoma pavo*) or day hauls (e.g.,  
 337 *Gymnammodytes cicereus*), representing just < 0.06 % of the total abundance.

338 **Table 2:** Different taxa occurring in the study area. **SOM code:** number assigned to each taxon in the  
 339 SOM figure (Figure 6). **TA:** Total abundance (ind 10 m<sup>-2</sup>) of each taxa; **RA:** Relative abundance %; **NL:**  
 340 Number of Class Lengths found for each taxa; **L Range:** Min and max measured length in mm; **%D:** % of  
 341 TA during day hauls; **%N:** % of TA during night hauls; **L Range D:** Length classes present in day hauls;  
 342 **L Range N:** Length classes present in night hauls; In bold: RA>1%. \*: Taxa with preflexion stages  
 343 included in the SOM (RA>0.2%); \*\*: Taxa with pre- and postflexion stages included in the SOM

Family	Lower taxa Identified	SO M code	TA	RA (%)	N ° L	L Range (mm)	%D	%N	L Range D	L Range N
Ammodytidae	<i>Gymnammodytes cicereus</i>		12.9	0.06	3	2.45-4.47	100.0	0.0	L2-L4	
Belonidae	<i>Belone belone</i>		1.4	0.01	0		100.0	0.0		
Blenniidae	Blenniidae		384.9	<b>1.71</b>	8	1.75-8.79	22.1	77.9	L1-L7	L1-L8
Bothidae	<i>Arnoglossus</i> spp.*	11	113.7	0.51	8	1.24-9.56	49.7	50.3	L1-L3. L5. L9	L1-L4. L6.L7
	<i>Bothus</i> spp.		29.6	0.13	3	1.54-3.35	4.6	95.4	L1	L1-L3
Callionymidae	Callionymidae*	17	60.9	0.27	3	1.25-3.73	67.5	32.5	L1-L3	L1-L3
Carangidae	<i>Seriola dumerili</i>		0.1	0.00	0		100.0	0.0		
Centracanthidae	<i>Trachurus</i> spp.*	6	403.2	<b>1.80</b>	4	1.27-4.13	22.9	77.1	L1-L3	L1-L4
	<i>Spicara flexuosa</i> *	7	225.9	<b>1.01</b>	5	1.59-5.85	33.2	66.8	L1-L5	L1-L5
	<i>Spicara smarís</i> **	1,23	6971.5	<b>31.0</b>	8	1.16-8.98	41.8	58.2	L1-L8	L1-L8
Cepolidae	<i>Cepola</i> spp.		1.4	0.01	0		0.0	0		
Clupeidae	<i>Sardinella aurita</i> **	3,24	1517.9	<b>6.76</b>	14	1.68-15	21.0	79.0	L1-L7. L9. L11	L2-L14
	<i>Coryphaena hippurus</i>		7.5	0.03	2	2.03-3.03	35.5	64.5	L2	L2. L3
Engraulidae	<i>Engraulis encrasicolus</i> **	2,25	3953.3	<b>17.6</b>	14	1.93-14.3	40.3	59.7	L1-L9	L2-L14
Gobiesocidae	Gobiesocidae		38.1	0.17	5	2.86-6.23	64.3	35.7	L2-L6	L3. L4
Gobiidae	Gobiidae		3008.4	<b>13.4</b>	8	1.16-7.63	27.7	72.3	L1-L6	L1-L7
Gonostomatidae	<i>Cyclothone braueri</i>		48.6	0.22	8	1.91-12.6	36.9	63.1	L3. L4. L6	L1-L5. L7. L12
	<i>Coris julis</i> *	10	200.8	0.89	4	1.38-4.15	14.6	85.4	L1-L3	L1-L4
Labridae	Labridae		777.5	<b>3.46</b>	5	1.29-5.17	55.6	44.4	L1-L5	L1-L4

	<i>Thalassoma pavo</i>				2.63-3.93	100.0				
	<i>Mullus barbatus*</i>	13	126.0	0.06	2	3.93	0.0	0		L2. L3
Mullidae	<i>Mullus surmuletus*</i>					1.83-2.43				L2-L5.
	<i>Ceratoscopelus maderensis*</i>	22	55.1	0.56	4	11.6	50.4	49.6	L1-L4	L11
Myctophidae	<i>Lampanyctus crocodilus</i>					2.96-6.52				L2-L5
	<i>Myctophum punctatum</i>	16	68.5	0.30	5	6.52	22.0	78.0	L3-L5	L2-L6
								100.		
								0.0		
								0		
Ophidiidae	Ophidiidae*	12	121.5	0.54	3	2.17-4.66	60.6	39.4	L2-L4	L2-L4
						4.25-4.62		0		
Paralepididae	Paralepididae					3.1	0.01	1		
	<i>Chromis chromis**</i>	4,26	599.6	<b>2.67</b>	5	1.37-5.44	26.4	73.6	L1-L4	L1-L5
Pomacentridae	<i>Auxis rochei*</i>	14	92.4	0.41	6	1.53-6.7	28.8	71.2	L1-L6	L1-L6
Scombridae	<i>Thunnus alalunga</i>							100.		
	<i>Thunnus thynnus</i>					1.9	0.01	0		0.0
	<i>Lepidorhombus boscii</i>					8.7	0.04	2		L4. L5
Scophthalmidae	<i>Scorpaena porcus*</i>	18	51.1	0.23	3	4.23-5.86	75.3	24.7	L4. L5	L5
	<i>Scorpaena spp.</i>					2.32-4.4				L5
						1.59-3.86				L5
Scorpaenidae						1.58-2.82				L1-L3
						1.67-1.78				L1. L2
Serranidae	<i>Anthias anthias</i>					4.4	0.02	1		L1. L2
	<i>Serranus hepatus*</i>	8	211.6	0.94	7	1.78-7.61	50.8	49.2	L1	L1
	<i>Serranus spp.*</i>	5	374.0	<b>1.67</b>	7	1.04-7.48	41.2	58.8	L1-L4.	L1-L7
						1.35-1.58			L6	L1-L7
Soleidae	Soleidae*	21	42.9	0.19	5	5.55-1.97	32.9	67.1	L1-L6	L1-L7
	<i>Boops boops*</i>	20	48.8	0.22	6	6.05	88.8	11.2	L1-L6	L1-L7
	<i>Diplodus spp.*</i>	9	199.2	0.89	8	1.35-12.6	47.2	52.8	L1-L3.	L1-L7
Sparidae	<i>Oblada melanura*</i>	15	123.8	0.55	5	2.21-6.87	35.8	64.2	L5	L2-L4
	<i>Pagrus pagrus*</i>	19	43.5	0.19	4	1.914,6	20.1	79.9	L2. L3	L2-L6
	Sparidae spp.					1.28-6.18	76.5	23.5	L1-L6	L1-L4
						1.78-5.88				L1-L3.
Sphyraenidae	Sphyraenidae					22.7	0.10	5		L2. L3.
										L5
								100.		
Sygnathidae	Sygnathidae					1.6	0.01	0		
								0		
								0.0		
Synodontidae	<i>Synodus saurus</i>					2.79-4.12				
						0.18				
						3				
								3.2		L3
								96.8		L1-L4
Trachinidae	<i>Trachinus draco</i>					1.96-52.1				
						0.23				
						4				
								36.1		L2-L4
								63.9		L1-L4
								100.		
Triglidae	Triglidae					1.38-7.8				L1. L3.
						0.03				L5
						3		0		
								0.0		
Unidentified	Unidentified					2146.				
						3	<b>9.56</b>	0		
								40.6		
								59.4		

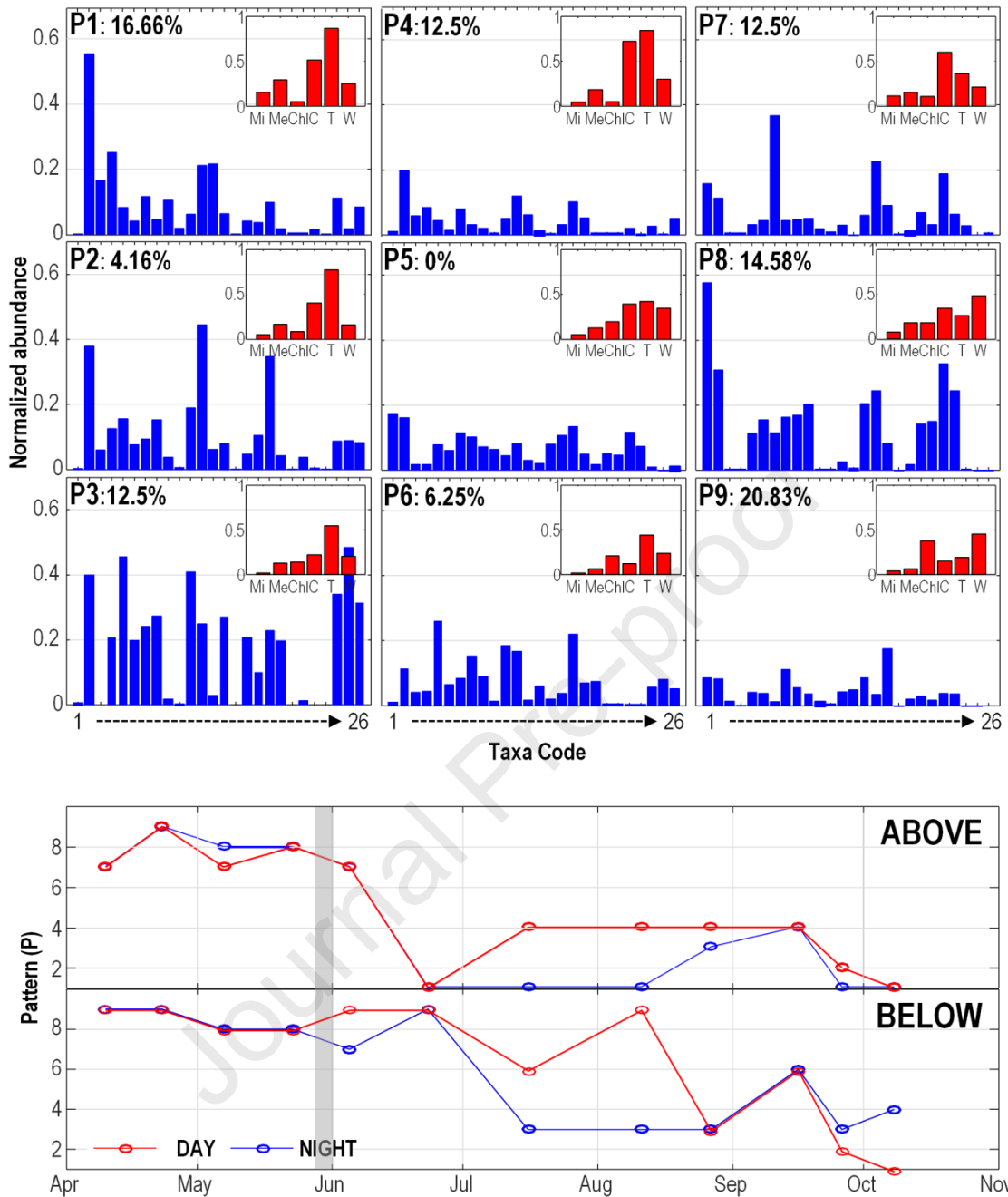
345 The wider length ranges were represented by clupeiform fish, which were also the most  
346 abundant; *E. encrasicolus* and *S. aurita* larvae ranged between 2.01 and 15 mm SL (L2-  
347 L14). The sparid *S. smaris*, also highly abundant, oscillated between 1.16-8.98 mm (L1-  
348 L9). Taxa collected in lower abundances presented fewer length classes, including the  
349 sparid *Pagrus pagrus* (L2, L3) or the myctophid *Cyclothone braueri* (L3, L4, L6, Table  
350 2). Univariate analyses were not attempted due to the high complexity of the data,  
351 including species-specific triggers of appearance in the plankton, non-independence of  
352 several factors, etc. (see Discussion).

353

#### 354 3.4. SOM analysis: patterns of the environment-LFA relationship

355 We used a coupled SOM analysis to extract general patterns of LFA response to  
356 environmental forcing below and above the thermocline, at different stages and taking  
357 into account temporal variability. Only taxa with abundances representing more than  
358 0.19% of the total abundance (22 taxa) were included in the SOM computations (Table  
359 2). The unidentified Gobiidae, Labridae, and Blenniidae families and the Sparidae spp.  
360 taxa were not used in this analysis as they comprise several taxa with possible different  
361 day/night patterns, reproductive cycle and different behaviour against stratification.  
362 Only *S. smaris*, *S. aurita*, *E. encrasicolus* and *C. chromis* had enough individuals at the  
363 post-flexion as to be included in the SOM analysis.

364 Figure 6 (top panel) shows the 9 patterns extracted from the 3x3 coupled SOM analysis  
365 of taxa abundances and environmental parameters, where the probability of finding that  
366 particular pattern in the data is indicated. The temporal succession of the different  
367 patterns is also displayed in the bottom panel. The topological ordering of the patterns  
368 in the neural network performed by SOM is clearly depicted: patterns with higher larval  
369 abundances, higher presence of post-flexion stages (taxa 23-26 in Fig. 6, see also Table  
370 2) and stronger influence of water temperature are located around the bottom-left corner  
371 of the neural network, and those with lower taxa abundances, absence of post-flexion  
372 stages and environmental scenarios characterized by the high velocity of the current and  
373 lower temperatures are located around the top-right corner. As a consequence of the  
374 preservation of topology, the closer to these extremes, the more similar the patterns are  
375 (e.g., pattern 2 (P2) is more similar to P1 than to P8). Patterns with the highest  
376 probability of occurrence are located in the corners of the neural networks being P9 the  
377 most dominant (ca. 21%) followed by P1, P8, P3, and P7. Note that P5 with zero  
378 probability of occurrence is included by SOM to preserve topological continuity.



379

380 **Figure 6:** Results of the SOM analysis. Top: Abundance distribution patterns of each taxa (ordered 1 to  
 381 26, Table 2) given by a 3x3 SOM analysis. Number in each pattern label (P1 to P9) is the corresponding  
 382 total occurrence probability. Inside each taxa pattern (blue), the corresponding environmental scenario  
 383 pattern (red). Bottom: Evolution of each taxa and environmental pattern shown in the top plot during the  
 384 study period. The shaded area represents the onset of stratification. Taxa numbers (Table 2): Pre-flexion  
 385 stages (1-22); Post-flexion stages (23-26); Environmental variables: Mi: Microzooplankton dry weight  
 386 (biomass,  $\text{mg m}^{-3}$ ); Me: Mesozooplankton dry weight (biomass,  $\text{mg m}^{-3}$ ); Chl: Chlorophyll ( $\text{mg m}^{-3}$ ); C:  
 387 module of the current ( $\text{m s}^{-1}$ ); T: water temperature ( $^{\circ}\text{C}$ ) and W: wave height (m)

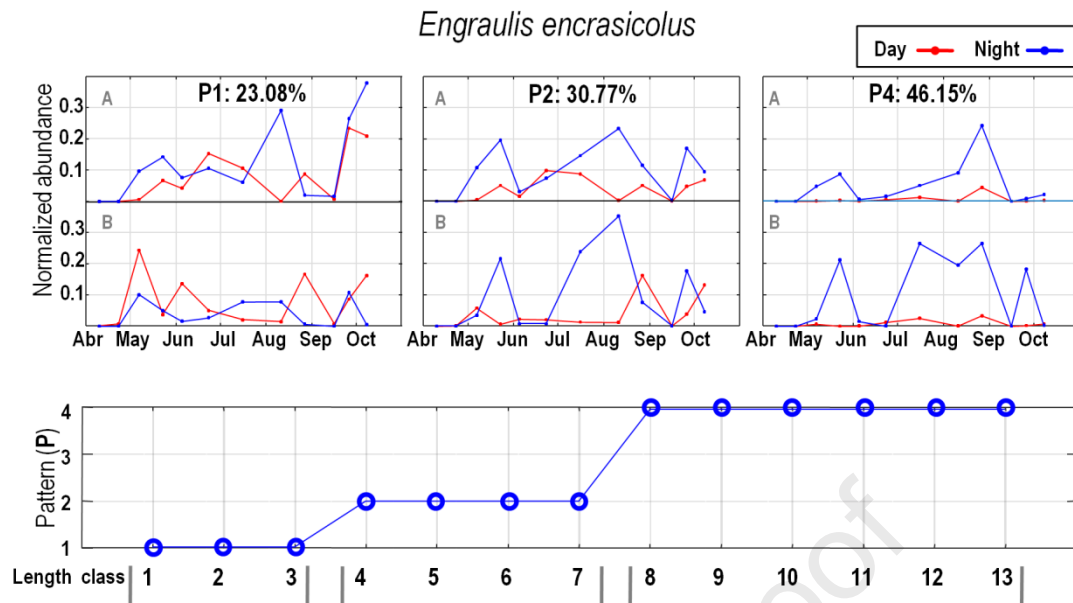
388 The temporal succession of the extracted patterns also follows the bottom-right to top-  
 389 left distribution (Fig. 6, bottom). That figure shows that minimum day-night differences  
 390 were observed above or below the thermocline before the onset of stratification (~

391 June). The patterns are grouped representing different situations occurring at different  
392 times, i.e., the group of nearby patterns (P7-P9) are more dominant from April to May,  
393 and patterns (P1-P6) dominate from June onwards, in coincidence with the development  
394 of the thermocline in the area (Figs 3 a, d). This transition implies that before the  
395 thermocline establishment, prevailing patterns are formed by few taxa and high  
396 abundances of *S. smaris*. Those taxa spawn at low temperatures and exploit a situation  
397 of high chlorophyll. On the contrary, after the thermocline is formed, high temperature,  
398 relatively low Chl-a and plankton food constitute the prevailing environmental  
399 conditions for P1-4. Noticeably, the SOM reveals, in the temporal evolution of the Best-  
400 Matching Units (BMUs), that samples taken during the day and above the thermocline  
401 in June-September (P4, and to a lesser extent P2 and P1) differ largely from the patterns  
402 emerging from below the thermocline; in general, the abundance of species above the  
403 thermocline during the more stratified period was lower than below the thermocline.  
404 Finally, post-flexion larvae (species 24-26, Fig. 6 top panel) appear fundamentally in P3  
405 and are detected mainly during the night and below the thermocline in July-August.

406

### 407 3.5. SOM application to single species evolution.

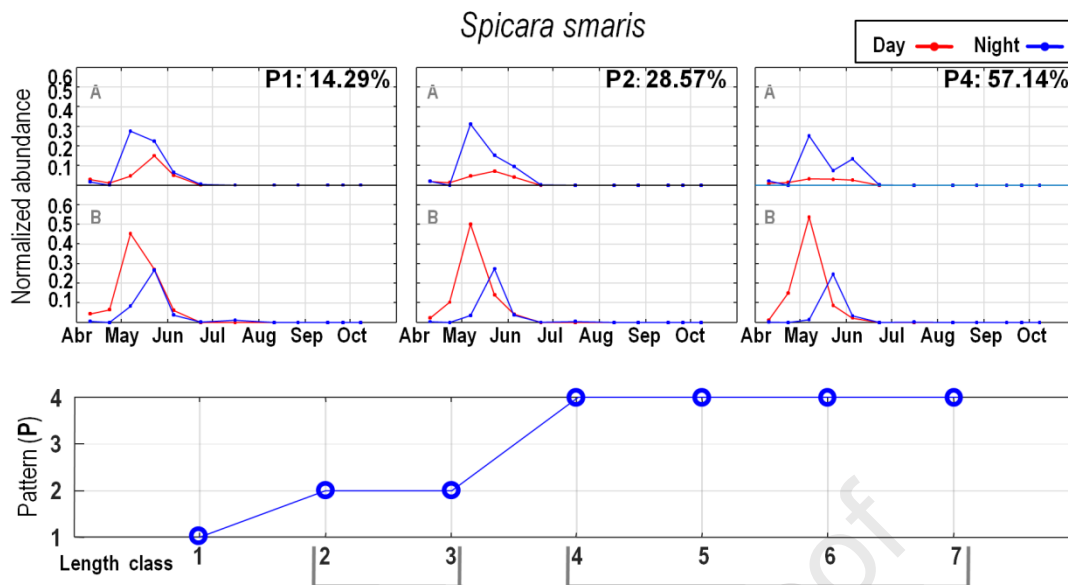
408 We here demonstrate the utility of SOM analyses for species for which enough detailed  
409 information (through time and length abundances) exists: the spring/summer-spawning  
410 European anchovy *E. encrasicolus* and the abundant winter-spawning sparid *S. smaris*.  
411 In these cases the input data used in the SOM computations is composed of time series  
412 of the abundance of a particular species for different size classes. The temporal patterns  
413 of all the *E. encrasicolus* and *S. smaris* length classes were analyzed separately through  
414 two 2x2 SOM. In the *E. encrasicolus* analysis, pattern 3 showed zero probability of  
415 being present among our data (Fig. 7). The pattern representing most data (P4, 46.15%)  
416 showed the trend of capturing more individuals during the night during all the time  
417 series, shared to a lesser extent by P1 and P2. Daytime larval abundances were higher in  
418 Pattern 1, with a 23% probability of being present in our data and corresponding mainly  
419 to the smallest individuals (L1 to L3, Fig. 7 bottom). A progressive reduction in the  
420 daytime presence of larvae in the tows is represented by Pattern 2, corresponding to  
421 length classes 4-7, whereas the largest size classes (L8-L13) are clearly captured  
422 basically in the night, according to P4 (Fig. 7, bottom).



423

424 **Figure 7:** Results of the SOM analysis for *E. encrasicolus* length classes. Top: Temporal patterns of *E.*  
 425 *encrasicolus* abundance above (A) and below (B) the thermocline given by a 2x2 SOM analysis during  
 426 the day (red) and night (blue). Number in each pattern label (P1 to P4) is the corresponding total  
 427 occurrence probability. Bottom: Correspondence of the patterns shown in the top plot to each of the  
 428 length classes.

429 The results of the SOM applied for *S. smarís* are shown in Fig. 8. In this case, pattern 3  
 430 showed no probabilities of being present among our data. The most probable pattern  
 431 (57.14%) was P4, followed by P2 (28.57%) and P1 (14.29%). The largest individuals  
 432 (length classes L4 to L7) followed P4, whose main differences with P1 and P2 (L1 to  
 433 L3) were lower abundances above the thermocline, but fundamentally a high  
 434 concentration below the thermocline during daylight, and not so much during the night.  
 435 On the contrary, they were almost absent above the thermocline during daylight. The  
 436 other patterns showed that for smaller larvae, this absence over the thermocline during  
 437 daylight was less pronounced.



438

439 **Figure 8:** Results of the SOM analysis for *S. smaris* length classes. Top: Temporal patterns of *S. smaris*  
 440 abundance above (A) and below (B) the thermocline given by a 2x2 SOM analysis during the day (red)  
 441 and night (blue). Number in each pattern label (P1 to P4) is the corresponding total occurrence  
 442 probability. Bottom: Correspondence of the patterns shown in the top plot to each of the length classes.

443

#### 444 4. DISCUSSION

445 The results of the present study revealed differences in the patterns of abundance and  
 446 vertical distribution of fish larvae before and after the establishment of the water  
 447 column stratification. The use of Self Organised Maps analysis (SOM) made possible  
 448 the reduction of the multiple non-linear relationships among taxa and environmental  
 449 variables into more understandable patterns of probability, showing that valuable  
 450 information can be extracted when applied to data sets of different complexity.

451 There are at least three drivers of complexity in the way to investigate our main  
 452 hypothesis of the vertical distribution of fish larvae being associated with the properties  
 453 of the environment. They are basically the natural turnover of taxa that follows  
 454 seasonality, the differences in behavior between ontogenetic stages of the same taxa,  
 455 and finally, the choice of the different environmental parameters that might influence  
 456 the processes. Trying to formally analyze how each species behaves with regard to these  
 457 factors would have probably implied the construction of several complex models (e.g.,  
 458 state-space models) for each species, given that typical GLMM or GAMS are  
 459 inappropriate due to the underlying properties of the data.

460 The succession of taxa in the area, characterized by a progressive change in assemblage  
 461 composition throughout spring, and a sharp change (mainly due to the increase of

462 benthopelagic species) in early summer were already described in the NW  
463 Mediterranean (Álvarez et al., 2012; Fernández de Puellas et al., 2007; Masó et al.,  
464 1998).

465 The seasonal differences detected before and after the onset of stratification, with higher  
466 abundances but lower number of taxa in spring, and an opposite pattern in summer are  
467 also in concordance with previous descriptions in the area (Álvarez et al., 2012;  
468 Fernández de Puellas et al., 2007). These differences in reproductive strategies between  
469 spring and summer assemblages have also been described for other areas in the  
470 Mediterranean such as the Catalan sea (Sabatés, 1990), northern Aegean Sea (Koutrakis  
471 et al., 2004) and also in distant areas such as the South China Sea (Huang et al., 2017).  
472 In general, the succession of taxa and differences in spawning strategies between taxa  
473 have been attributed to the reduction of inter- and intra-specific competition for food  
474 resources in the NW Mediterranean (Sabatés et al., 2007), and more specifically to  
475 shifts in the prevailing trophic pathway exploited by reproductive adults; from a more  
476 productive pelagic environment during spring, vs. a more productive benthic  
477 environment (rocky bottom and seagrass meadows) in summer (Álvarez et al., 2012).

478 Most larvae in our study were small and undeveloped due to i) the sampling method  
479 (Bongo-40), which selects for mainly preflexion stages (Catalán et al., 2014) and ii) the  
480 fact that Palma Bay is a productive spawning ground for many species (Álvarez et al.,  
481 2015a, 2012). Due to the limitation in size classes, the analysis of ontogenetic-  
482 dependent migration (e.g., Borges et al., 2007; Huebert et al., 2011; Irisson et al., 2009)  
483 could only be tested for few species. However, the potential of SOM for this type of  
484 analysis is clear, particularly for the combined use of non-linear methods and the use of  
485 probabilistic proxies in the interpretation.

486 The division into pre and post notochord flexion, used to differentiate among swimming  
487 abilities and widely applied in the literature (Olivar et al., 2018; Olivar and Sabatés,  
488 1997, among others), has been proven not to be the best criterion to depict vertical  
489 positioning, as revealed by the two SOM analysis conducted on individual taxa (Figs 7  
490 and 8). For *Spicara smaris*, the literature proposed 5.5 mm SL as flexion length (Table  
491 1, Alemany, 1997) whilst we found differences in the vertical behavior after the 3 mm  
492 (Fig. 8). In the *Engraulis encrasicolus* case, 10 mm SL was used to group individuals  
493 into pre and post flexion (Table 1, Somarakis and Nikolioudakis, 2010). However, in  
494 the SOM analysis, three different size patterns with respect to the thermocline were  
495 recognized: 1-3 mm, 4-7 mm, and 8-13 mm (Fig. 7). The onset of the notochord flexion

496 in European anchovy was determined around 7 mm SL of preserved length by  
497 Somarakis and Nikolioudakis (2010) and was related to the initiation of swim-bladder  
498 inflation (considered to trigger the onset of vertical migrations and subsequent  
499 schooling behavior). Our results suggest that SOM can be a useful method to  
500 summarize vertical distribution data through time and ontogeny. However, the full  
501 power of SOM would be further revealed in even more complex data sets, for example,  
502 using fine-scale image-based vertical sampling techniques. In this respect, artificial  
503 intelligence that uses complex neural network approaches (e.g., Deep Learning) is  
504 irrupting in the analyses of larval fish ecology (e.g., Axler et al., 2020; Catalán et al.,  
505 2020).

506 The wide variety of environmental variables that can influence the vertical position of  
507 fish larvae, added to the potential non-linearity of their possible influence, makes the  
508 statistical or numerical approximations to the problem an uphill climb. Most of the  
509 research in the vertical position of fish larvae is thus centered on the description of the  
510 environment and the larval fish associations and the discussion of possible relationships  
511 among them (e.g. Muhling and Beckley, 2007; Sánchez-Velasco et al., 2007). Some  
512 authors have addressed their research in a numerical way, with correlation coefficients  
513 (Gray and Kingsford, 2003; Rodríguez et al., 2006) and multiple linear regression  
514 (Vargas-Yáñez and Sabatés, 2007). We show that the SOM analysis can be a useful tool  
515 to handle both the high number of variables and the nonlinearity of the processes under  
516 analysis. The application of the current analysis, however, does not preclude the need to  
517 conduct a priori elimination of confounding variables.

518 Both dependence and independence of vertical distributions from the water column's  
519 vertical thermal structure have been observed for coastal and oceanic waters in different  
520 regions of the world. As an example, the relationship between the vertical distribution  
521 of fish larvae and the seasonal evolution of the structure of the water column was  
522 studied using static stability and the pycnocline position as a stratification indicator in  
523 Bahia de La Paz, SW Gulf of California (Sánchez-Velasco et al., 2007). The authors  
524 concluded that significant differences in taxa and larval abundances were found among  
525 the water column's most stable stratum and the below-pycnocline stratum. Our results  
526 support those findings, with differences found before and after the stratification period  
527 in the area, with most of the species found in the stratified (stable) period.

528 However, Rodríguez et al. (2006) reported an almost negligible influence of the  
529 thermocline on the vertical distribution of fish larvae in the Canary-African coastal

530 transition zone and related that result to the relatively weak thermocline in the area.  
531 Gray and Kingsford (2003) also provided evidence that thermoclines had no detectable  
532 effect on vertical distributions of fish larvae and mesozooplankton in dynamic coastal  
533 waters, although in that case, perturbations in the position and intensity of thermoclines  
534 were frequent. Laboratory studies on the effect of vertical gradients on larval fish  
535 distribution show that the thermocline can exert a variable effect depending on the  
536 species, stage, and other variables such as fish condition or visibility (Catalán et al.,  
537 2011; Reglero et al., 2018; Vollset et al., 2013).

538 When analyzed together, all studies seem to converge at one point: stability of the water  
539 column in terms of mixing activity conditions can be related to the vertical position of  
540 fish larvae (here, larval behavior plays a more prominent role), whereas the lack of  
541 stability (e.g. weak or perturbed thermocline) weakens the detection of patterns at the  
542 vertical scale. The behavioral control will, in turn, be dependent on larval swimming  
543 capacities (e.g., Olivar et al., 2001; Ospina-Alvarez et al., 2012). Siegel et al., (2008)  
544 concluded that larval settlement is inherently a stochastic process driven by the  
545 interaction between coastal circulations and organism life histories. Siegel's "settlement  
546 equation" (coastal circulations; organism life histories) can be seen as a balance  
547 between its terms, depending on the moment in which the system is observed: coastal  
548 circulation might gain prominence for settlement in unstable scenarios (spring mixed  
549 column water in our study) whereas the influence of the organism life histories on  
550 settlement gains weight in stable scenarios (summer stratification period in our study).  
551 Although the sampling of a unique station throughout time was used to assume  
552 stationary conditions in our study, the influence of dynamical processes induced by  
553 lateral and vertical stirring, vertical shear of horizontal velocities, and advection of  
554 larvae cannot be discarded, adding complexity to the system. Other hypotheses confer a  
555 relevant role to larval behavior and justify the need for vertically-resolved surveys: the  
556 Sense Acuity and Behavioral hypothesis (Teodósio et al., 2016) proposes that  
557 individuals develop different behaviors and skills depending on the coastal cues they  
558 face. The importance of behavior for Mediterranean fish was recently proved by.

559 Summarizing, we could determine differences in the vertical strategies of fish larval  
560 assemblages before and after the establishment of the stratified period in a very complex  
561 data set through the use of an automatic data-analysis method (Self Organizing Map,  
562 SOM). The method neither generates cause-effect relationships nor extracts species-  
563 specific patterns (unless specified, as shown in some examples) in the way it has been

564 applied. However, SOM analysis allowed the description of the whole multispecific  
 565 system overcoming the difficulties inherent in describing non linear processes. The  
 566 possibility of analyzing these intricate multivariate patterns without the restriction of  
 567 linear approaches is a useful tool in understanding the complexity of recruitment  
 568 processes and settlement success of fish.

569

## 570 **5. Acknowledgements**

571 This work was funded by the Spanish Ministry of Economy and Competitiveness (Ref:  
 572 CTM2012-39476-C02-01). The same funding scheme partially supported I.C. through  
 573 the project REC2 (Ref: CTM2011-23835). J.S. F-M. received a French state aid  
 574 managed by the National Research Agency under the ISblue program (ANR-17-EURE-  
 575 0015). I.H-C. acknowledges the Vicenç Mut grant funded by the Government of the  
 576 Balearic Islands, Spain, and the European Social Fund (ESF) Operational Programme.  
 577 C.D.G. was funded by a fellowship (FPI-INIA-2012) from the National Institute of  
 578 Agricultural and Food Research and Technology. P.M. S-H. was supported by a Ph.D.  
 579 research fellowship FPI (Formación Personal Investigación) fellowship BES-2013-  
 580 067305 from MINECO. We thank Dr. G. Basterretxea for his help during the  
 581 elaboration of this work.

## 582 **6. REFERENCES**

- 583 Alemany, F., 1997. Ictioplankton del Mar Balear. PhD Thesis. Universitat de les Illes  
 584 Balears.
- 585 Alós, J., Palmer, M., Catalan, I.A., Alonso-Fernández, A., Basterretxea, G., Jordi, A.,  
 586 Buttay, L., Morales-Nin, B., Arlinghaus, R., 2014. Selective exploitation of  
 587 spatially structured coastal fish populations by recreational anglers may lead to  
 588 evolutionary downsizing of adults. *Mar. Ecol. Prog. Ser.* 503, 219–233.  
 589 <https://doi.org/10.3354/meps10745>
- 590 Álvarez, I., Catalán, I.A., Jordi, A., Alemany, F., Basterretxea, G., 2015a. Interaction  
 591 between spawning habitat and coastally steered circulation regulate larval fish  
 592 retention in a large shallow temperate bay. *Estuar. Coast. Shelf Sci.* 167, 377–389.  
 593 <https://doi.org/10.1016/j.ecss.2015.10.015>
- 594 Álvarez, I., Catalán, I.A., Jordi, A., Palmer, M., Sabatés, A., Basterretxea, G., 2012.  
 595 Drivers of larval fish assemblage shift during the spring-summer transition in the  
 596 coastal Mediterranean. *Estuar. Coast. Shelf Sci.* 97, 127–135.  
 597 <https://doi.org/10.1016/j.ecss.2011.11.029>

- 598 Álvarez, I., Rodríguez, J.M., Catalán, I.A., Hidalgo, M., Álvarez-Berastegui, D., Balbín,  
599 R., Aparicio-González, A., Alemany, F., 2015b. Larval fish assemblage structure  
600 in the surface layer of the northwestern Mediterranean under contrasting  
601 oceanographic scenarios. *J. Plankton Res.* 37.  
602 <https://doi.org/10.1093/plankt/fbv055>
- 603 Arvola, L., Rask, M., Forsius, M., Ala-Opas, P., Keskitalo, J., Kulo, K., Kurkilahti, M.,  
604 Lehtovaara, A., Sairanen, S., Salo, S., Saloranta, T., Verta, M., Vesala, S., 2017.  
605 Food web responses to artificial mixing in a small boreal lake. *Water (Switzerland)*  
606 9, 1–21. <https://doi.org/10.3390/w9070515>
- 607 Axler, K.E., Sponaugle, S., Briseño-Avena, C., Jr, H.F., Warner, S.J., Dzwonkowski,  
608 B., Dykstra, S.L., Cowen, R.K., 2020. Fine-scale larval fish distributions and  
609 predator-prey dynamics in a coastal river-dominated ecosystem. *Mar. Ecol. Prog.*  
610 *Ser.* 650, 37–61.
- 611 Basterretxea, G., Font-Muñoz, J.S., Salgado-Hernanz, P.M., Arrieta, J., Hernández-  
612 Carrasco, I., 2018. Patterns of chlorophyll interannual variability in Mediterranean  
613 biogeographical regions. *Remote Sens. Environ.* 215, 7–17.  
614 <https://doi.org/10.1016/j.rse.2018.05.027>
- 615 Basterretxea, G., Jordi, A., Catalán, I.A., Sabates, A., 2012. Model-based assessment of  
616 local-scale fish larval connectivity in a network of marine protected areas. *Fish.*  
617 *Oceanogr.* 21, 291–306. <https://doi.org/10.1111/j.1365-2419.2012.00625.x>
- 618 Bensoussan, N., Romano, J.C., Harmelin, J.G., Garrabou, J., 2010. High resolution  
619 characterization of northwest Mediterranean coastal waters thermal regimes: To  
620 better understand responses of benthic communities to climate change. *Estuar.*  
621 *Coast. Shelf Sci.* 87, 431–441. <https://doi.org/10.1016/j.ecss.2010.01.008>
- 622 Borges, R., Beldade, R., Gonçalves, E.J., 2007. Vertical structure of very nearshore  
623 larval fish assemblages in a temperate rocky coast. *Mar. Biol.* 151, 1349–1363.  
624 <https://doi.org/10.1007/s00227-006-0574-z>
- 625 Catalán, I., Vollset, K.W., Morales-Nin, B., Folkvord, A., 2011. The effect of  
626 temperature gradients and stomach fullness on the vertical distribution of larval  
627 herring in experimental columns. *J. Exp. Mar. Bio. Ecol.* 404, 26–32.  
628 <https://doi.org/10.1016/j.jembe.2011.05.005>
- 629 Catalán, I.A., Dunand, A., Álvarez, I., Alós, J., Colinas, N., Nash, R.D.M., 2014. An  
630 evaluation of sampling methodology for assessing settlement of temperate fish in  
631 seagrass meadows. *Mediterr. Mar. Sci.* 15. <https://doi.org/10.12681/mms.539>

- 632 Catalán, I.A., Reglero, P., Álvarez, I., 2020. Research on early life stages of fish: A  
633 lively field. *Mar. Ecol. Prog. Ser.* 650. <https://doi.org/10.3354/meps13491>
- 634 Cianelli, L., Bailey, K., Olsen, E.M., 2015. Evolutionary and ecological constraints of  
635 fish spawning habitats. *ICES J. Mar. Sci.* 72, 285–296.  
636 <https://doi.org/10.4135/9781412953924.n678>
- 637 Coma, R., Ribes, M., Serrano, E., Jimenez, E., Salat, J., Pascual, J., 2009. Global  
638 warming-enhanced stratification and mass mortality events in the Mediterranean.  
639 *Proc. Natl. Acad. Sci.* 106, 6176–6181. <https://doi.org/10.1073/pnas.0805801106>
- 640 Ditty, J.G., Shaw, R.F., Grimes, C.B., Cope, J.S., 1994. Larval development,  
641 distribution, and abundance of common dolphin, *Coryphaena hippurus*, and  
642 pompano dolphin, *C. equiselis* (family: Coryphaenidae), in the northern Gulf of  
643 Mexico. *Fish. Bull.* 92, 275–291.
- 644 Fernández de Puellas, M.L., Alemany, F., Jansá, J., 2007. Zooplankton time-series in  
645 the Balearic Sea (Western Mediterranean): Variability during the decade 1994-  
646 2003. *Prog. Oceanogr.* 74, 329–354. <https://doi.org/10.1016/j.pocean.2007.04.009>
- 647 Font-Muñoz, J.S., Jordi, A., Anglès, S., Ferriol, P., Garcés, E., Basterretxea, G., 2018.  
648 Assessing phytoplankton community composition using combined pigment and  
649 particle size distribution analysis. *Mar. Ecol. Prog. Ser.* 594, 51–63.  
650 <https://doi.org/10.3354/meps12559>
- 651 Gray, C.A., Kingsford, M.J., 2003. Variability in thermocline depth and strength, and  
652 relationships with vertical distributions of fish larvae and mesozooplankton in  
653 dynamic coastal waters. *Mar. Ecol. Prog. Ser.* <https://doi.org/10.3354/meps247211>
- 654 Hernández-Carrasco, I., Orfila, A., 2018. The Role of an Intense Front on the  
655 Connectivity of the Western Mediterranean Sea: The Cartagena-Tenes Front. *J.*  
656 *Geophys. Res. Ocean.* 123, 4398–4422. <https://doi.org/10.1029/2017JC013613>
- 657 Hernández-Carrasco, I., Solabarrieta, L., Rubio, A., Esnaola, G., Reyes, E., Orfila, A.,  
658 2018. Impact of HF radar current gap-filling methodologies on the Lagrangian  
659 assessment of coastal dynamics. *Ocean Sci.* 14, 827–847.  
660 <https://doi.org/10.5194/os-14-827-2018>
- 661 Hjort, J., 1926. Fluctuations in the year classes of important foodfishes. *J. du Con-seil*  
662 *Int. pour l'Exploration la Mer* 1, 5–38.
- 663 Hjort, J., 1914. Fluctuations in the great fisheries of northern Europe viewed in the  
664 light of biological research. *Rapp. Procès-Verbaux des Réunions du Cons. Inter-*  
665 *national pour l'Exploration la Mer* 20, 1–228.

- 666 Houde, E.D., 2008. Emerging from Hjort's shadow. *J. Northwest Atl. Fish. Sci.* 41, 53–  
667 70. <https://doi.org/10.2960/J.v41.m634>
- 668 Houde, E.D., Schekter, R.C., 1980. Feeding by marine fish larvae: developmental and  
669 functional responses. *Environ. Biol. Fishes* 5, 315–334.  
670 <https://doi.org/10.1007/BF00005186>
- 671 Huang, D., Zhang, X., Jiang, Z., Zhang, J., Arbi, I., Jiang, X., Huang, X., Zhang, W.,  
672 2017. Seasonal fluctuations of ichthyoplankton assemblage in the northeastern  
673 South China Sea influenced by the Kuroshio intrusion. *J. Geophys. Res. Ocean.*  
674 *Res.* 122, 7253–7266. <https://doi.org/10.1002/2017JC013313>
- 675 Huebert, K.B., Cowen, R.K., Sponaugle, S., 2011. Vertical migrations of reef fish  
676 larvae in the straits of florida and effects on larval transport. *Limnol. Oceanogr.* 56,  
677 1653–1666. <https://doi.org/10.4319/lo.2011.56.5.1653>
- 678 Irisson, J.-O., Paris, C.B., Guigand, C.C., Planes, S., Org, I., 2009. Vertical distribution  
679 and ontogenetic 'migration' in coral reef fish larvae. *Mar. Biol.* 55, 1–29.  
680 <https://doi.org/10.43119/lo2009.55.2.0909>
- 681 Kingsford, M., Shanks, A.L., Morgan, S.G., Pineda, J., 2002. Sensory environments,  
682 larval abilities and local self recruitment. *Bull. Mar. Sci.* 70, 309–340.
- 683 Kohonen, T., 1997. *Self-Organizing Maps*. Springer Series in Information Sciences.
- 684 Kohonen, T., 1982. Self-organized formation of topologically correct feature maps.  
685 *Biol. Cybern.* 43, 59–69. <https://doi.org/10.1007/BF00337288>
- 686 Kolczynski, W.C., Hacker, J.P., 2014. The potential for self-organizing maps to identify  
687 model error structures. *Mon. Weather Rev.* 142, 1688–1696.  
688 <https://doi.org/10.1175/MWR-D-13-00189.1>
- 689 Koutrakis, E.T., Kallianiotis, A.A., Tsikliras, A.C., 2004. Temporal patterns of larval  
690 fish distribution and abundance in a coastal area of northern Greece \*. *Sci. Mar.*  
691 68, 585–595. <https://doi.org/10.3989/scimar.2004.68n4585>
- 692 Leis, J.M., 2006. Are Larvae of Demersal Fishes Plankton or Nekton?. *Adv Mar Biol*  
693 51, 58–141.
- 694 Leis, J.M., 1986. Vertical and horizontal distribution of fish larvae near coral reefs at  
695 Lizard Island, Great Barrier Reef. *Mar. Biol.* 90, 505–516.
- 696 Leis, J.M., Trnski, T., Dufour, V., Harmelin-Vivien, M., Renon, J.P., Galzin, R., 2003.  
697 Local completion of the pelagic larval stage of coastal fishes in coral-reef lagoons  
698 of the Society and Tuamotu Islands. *Coral Reefs* 22, 271–290.  
699 <https://doi.org/10.1007/s00338-003-0316-3>

- 700 Liu, Y., Weisberg, R.H., Mooers, C.N.K., 2006. Performance evaluation of the self-  
701 organizing map for feature extraction. *J. Geophys. Res. Ocean.* 111, 1–14.  
702 <https://doi.org/10.1029/2005JC003117>
- 703 Mann, K.H., Lazier, J.R.N., 1991. Dynamics of marine ecosystems: biological physical  
704 interactions in the oceans, *Dynamics of Marine Ecosystems*, Wiley Online Books.  
705 Blackwell Scientific Publications, Boston, MA.  
706 <https://doi.org/https://doi.org/10.1002/9781118687901.fmatter>
- 707 Masó, M., Sabatés, A., Pilar Olivar, M., 1998. Short-term physical and biological  
708 variability in the shelf-slope region of the NW Mediterranean during the spring  
709 transition period. *Cont. Shelf Res.* 18, 661–675. [https://doi.org/10.1016/S0278-](https://doi.org/10.1016/S0278-4343(98)00011-9)  
710 [4343\(98\)00011-9](https://doi.org/10.1016/S0278-4343(98)00011-9)
- 711 McBride, R.S., Fahay, M.P., Able, K.W., 2002. Larval and settlement periods of the  
712 northern searobin (*Prionotus carolinus*) and the striped searobin (*P. evolans*). *Fish.*  
713 *Bull.* 100, 63–73. <https://doi.org/10.1111/j.1439-0485.2006.00146.x>
- 714 Montgomery, J.C., Tolimieri, N., Haine, O.S., 2001. Active habitat selection by pre-  
715 settlement reef fishes. *Fish Fish.* 2, 261–277. [https://doi.org/10.1046/j.1467-](https://doi.org/10.1046/j.1467-2960.2001.00053.x)  
716 [2960.2001.00053.x](https://doi.org/10.1046/j.1467-2960.2001.00053.x)
- 717 Mörchen, F., Ultsch, A., 2005. Discovering temporal knowledge in multivariate time  
718 series, in: *Studies in Classification, Data Analysis, and Knowledge Organization*.  
719 pp. 272–279. <https://doi.org/10.1007/3-540-28084-7-30>
- 720 Muhling, B.A., Beckley, L.E., 2007. Seasonal variation in horizontal and vertical  
721 structure of larval fish assemblages off south-western Australia, with implications  
722 for larval transport. *J. Plankton Res.* 29, 967–983.  
723 <https://doi.org/10.1093/plankt/fbm072>
- 724 Nash, R.D.M., Geffen, A.J., 2012. Mortality through the early life-history of fish: What  
725 can we learn from European plaice (*Pleuronectes platessa* L.)? *J. Mar. Syst.* 93,  
726 58–68. <https://doi.org/10.1016/j.jmarsys.2011.09.009>
- 727 Nøttestad, L., Diaz, J., Pena, H., Sjøiland, H., Huse, G., Ferno, A., 2016. Feeding  
728 strategy of mackerel in the Norwegian Sea relative to currents, temperature, and  
729 prey. *Leif* 73, 1127–1137.
- 730 Olivar, M.P., Contreras, T., Hulley, P.A., Emelianov, M., López-Pérez, C., Tuset, V.,  
731 Castellón, A., 2018. Variation in the diel vertical distributions of larvae and  
732 transforming stages of oceanic fishes across the tropical and equatorial Atlantic.  
733 *Prog. Oceanogr.* <https://doi.org/10.1016/j.pocean.2017.12.005>

- 734 Olivar, M.P., Sabatés, A., 1997. Vertical distribution of fish larvae in the north-west  
735 Mediterranean Sea in spring. *Mar. Biol.* 129, 289–300.  
736 <https://doi.org/10.1007/s002270050169>
- 737 Olivar, M.P., Sabatés, A., Alemany, F., Balbín, R., Fernández de Puellas, M.L., Torres,  
738 A.P., 2014. Diel-depth distributions of fish larvae off the Balearic Islands (western  
739 Mediterranean) under two environmental scenarios. *J. Mar. Syst.* 138, 127–138.  
740 <https://doi.org/10.1016/j.jmarsys.2013.10.009>
- 741 Olivar, M.P., Salat, J., Palomera, I., 2001. Comparative study of spatial distribution  
742 patterns of the early stages of anchovy and pilchard in the NW Mediterranean Sea.  
743 *Mar. Ecol. Prog. Ser.* 217, 111–120. <https://doi.org/10.3354/meps217111>
- 744 Ospina-Alvarez, A., Parada, C., Palomera, I., 2012. Vertical migration effects on the  
745 dispersion and recruitment of European anchovy larvae: From spawning to nursery  
746 areas. *Ecol. Modell.* 231, 65–79. <https://doi.org/10.1016/j.ecolmodel.2012.02.001>
- 747 Paris, C.B., Cowen, R.K., 2004. Direct evidence of a biophysical retention mechanism  
748 for coral reef fish larvae. *Limnol. Oceanogr.* 49, 1964–1979.  
749 <https://doi.org/10.4319/lo.2004.49.6.1964>
- 750 Ramos, S., Ré, P., Bordalo, A.A., 2010. Recruitment of flatfish species to an estuarine  
751 nursery habitat (Lima estuary, NW Iberian Peninsula). *J. Sea Res.* 64, 473–486.  
752 <https://doi.org/10.1016/j.seares.2010.01.010>
- 753 Ré, P., Meneses, I., 2009. Early stages of marine fishes occurring in the Iberian  
754 Peninsula. Lisbon.
- 755 Reglero, P., Ortega, A., Balbín, R., Abascal, F.J., Medina, A., Blanco, E., de la  
756 Gándara, F., Alvarez-Berastegui, D., Hidalgo, M., Rasmuson, L., Alemany, F.,  
757 Fiksen, Ø., 2018. Atlantic bluefin tuna spawn at suboptimal temperatures for their  
758 offspring. *Proc. R. Soc. B Biol. Sci.* <https://doi.org/10.1098/rspb.2017.1405>
- 759 Richards, W.J., 2006. Early stages of Atlantic fishes: an identification guide for the  
760 western central north Atlantic. CRC Press.
- 761 Rodríguez, J.M., Gonzalez-Pola, C., Lopez-Urrutia, A., Nogueira, E., 2011.  
762 Composition and daytime vertical distribution of the ichthyoplankton assemblage  
763 in the central cantabrian Sea shelf, during summer: An eulerian study. *Cont. Shelf*  
764 *Res.* 31, 1462–1473. <https://doi.org/10.1016/j.csr.2011.06.007>
- 765 Rodríguez, J.M., Hernández-León, S., Barton, E.D., 2006. Vertical distribution of fish  
766 larvae in the Canaries-African coastal transition zone in summer. *Mar. Biol.* 149,  
767 885–897. <https://doi.org/10.1007/s00227-006-0270-z>

- 768 Ropke, A., 1993. Do larvae of mesopelagic fishes in the Arabian Sea adjust their  
769 vertical distribution to physical and biological gradients. *Mar. Ecol. Prog. Ser.* 101,  
770 223–236. <https://doi.org/10.3354/meps101223>
- 771 Russo, T., Scardi, M., Cataudella, S., 2014. Applications of self-organizing maps for  
772 ecomorphological investigations through early ontogeny of fish. *PLoS One* 9.  
773 <https://doi.org/10.1371/journal.pone.0086646>
- 774 Sabatés, A., 2004. Diel vertical distribution of fish larvae during the winter-mixing  
775 period in the Northwestern Mediterranean. *ICES J. Mar. Sci.* 61, 1243–1252.  
776 <https://doi.org/10.1016/j.icesjms.2004.07.022>
- 777 Sabatés, A., 1990. Changes in the heterogeneity of mesoscale distribution patterns of  
778 larval fish associated with a shallow coastal haline front. *Estuar. Coast. Shelf Sci.*  
779 30, 131–140. [https://doi.org/10.1016/0272-7714\(90\)90059-Z](https://doi.org/10.1016/0272-7714(90)90059-Z)
- 780 Sabatés, A., 1989. Sistemática y distribución espacio-temporal del ictioplancton en la  
781 costa catalana. PhD Thesis. Universitat de Barcelona.
- 782 Sabatés, A., Olivar, M.P., Salat, J., Palomera, I., Alemany, F., 2007. Physical and  
783 biological processes controlling the distribution of fish larvae in the NW  
784 Mediterranean. *Prog. Oceanogr.* 74, 355–376.  
785 <https://doi.org/10.1016/j.pocean.2007.04.017>
- 786 Sánchez-Velasco, L., Jiménez-Rosenberg, S.P.A., Lavín, M.F., 2007. Vertical  
787 distribution of fish larvae and its relation to water column structure in the  
788 southwestern Gulf of California. *Pacific Sci.* 61, 533–548.  
789 [https://doi.org/10.2984/1534-6188\(2007\)61\[533:VDOFLA\]2.0.CO;2](https://doi.org/10.2984/1534-6188(2007)61[533:VDOFLA]2.0.CO;2)
- 790 Schneider, C.A., Rasband, W.S., Eliceiri, K.W., 2012. NIH Image to ImageJ: 25 years  
791 of image analysis. *Nat. Methods* 9, 671–675. <https://doi.org/10.1038/nmeth.2089>
- 792 Schreck, T., 2010. Visual-Interactive Analysis With Self-Organizing Maps - Advances  
793 and Research Challenges. *Self-Organizing Maps*. <https://doi.org/10.5772/9171>
- 794 Sharon, I., Morowitz, M.J., Thomas, B.C., Costello, E.K., Relman, D.A., Banfield, J.F.,  
795 2013. Time series community genomics analysis reveals rapid shifts in bacterial  
796 species, strains, and phage during infant gut colonization. *Genome Res.* 23, 111–  
797 120. <https://doi.org/10.1101/gr.142315.112>
- 798 Siegel, D.A., Mitarai, S., Costello, C.J., Gaines, S.D., Kendall, B.E., Warner, R.R.,  
799 Winters, K.B., 2008. The stochastic nature of larval connectivity among nearshore  
800 marine populations. *Proc. Natl. Acad. Sci.* 105, 8974–8979.  
801 <https://doi.org/10.1073/pnas.0802544105>

- 802 Sinclair, M., Iles, T.D., 1985. Atlantic Herring (*Clupea harengus*) Distributions in the  
803 Gulf of Maine – Scotian Shelf Area in Relation to Oceanographic Features. Can. J.  
804 Fish. Aquat. Sci. 42, 880–887. <https://doi.org/10.1139/f85-112>
- 805 Smith, K.A., Gibbs, M.T., Middleton, J.H., Suthers, I.M., 1999. Short term variability in  
806 larval fish assemblages of the Sydney shelf: Tracers of hydrographic variability.  
807 Mar. Ecol. Prog. Ser. 178, 1–15. <https://doi.org/10.3354/meps178001>
- 808 Somarakis, S., Nikolioudakis, N., 2010. What makes a late anchovy larva? the  
809 development of the caudal fin seen as a milestone in fish ontogeny. J. Plankton  
810 Res. 32, 317–326. <https://doi.org/10.1093/plankt/fbp132>
- 811 Sponaugle, S., Cowen, R.K., Shanks, A., Morgan, S.G., Leis, J.M., Pineda, J., Boehlert,  
812 G.W., Kingsford, M.J., Lindeman, K.C., Grimes, C., Munro, J.L., 2002. Predicting  
813 self-recruitment in marine populations: Biophysical correlates and mechanisms.  
814 Bull. Mar. Sci. 70, 341–375. <https://doi.org/10.1016/j.csr.2006.01.020>
- 815 Teodósio, M.A., Paris, C.B., Wolanski, E., Morais, P., 2016. Biophysical processes  
816 leading to the ingress of temperate fish larvae into estuarine nursery areas: A  
817 review. Estuar. Coast. Shelf Sci. <https://doi.org/10.1016/j.ecss.2016.10.022>
- 818 Tojeira, I., Faria, A.M., Henriques, S., Faria, C., Gonçalves, E.J., 2012. Early  
819 development and larval behaviour of two clingfishes, *Lepadogaster purpurea* and  
820 *Lepadogaster lepadogaster* (Pisces: Gobiesocidae). Environ. Biol. Fishes 93, 449–  
821 459. <https://doi.org/10.1007/s10641-011-9935-7>
- 822 Vargas-Yáñez, M., Sabatés, A., 2007. Mesoscale high-frequency variability in the  
823 Alboran Sea and its influence on fish larvae distributions. J. Mar. Syst. 68, 421–  
824 438. <https://doi.org/10.1016/j.jmarsys.2007.01.004>
- 825 Vatanen, T., Osmala, M., Raiko, T., Lagus, K., Sysi-Aho, M., Orešič, M., Honkela, T.,  
826 Lähdesmäki, H., 2015. Self-organization and missing values in SOM and GTM.  
827 Neurocomputing 147, 60–70. <https://doi.org/10.1016/j.neucom.2014.02.061>
- 828 Vikebø, F., Sundby, S., Ådlandsvik, B., Fiksen, Ø., 2005. The combined effect of  
829 transport and temperature on distribution and growth of larvae and pelagic  
830 juveniles of Arcto-Norwegian cod. ICES J. Mar. Sci. 62, 1375–1386.  
831 <https://doi.org/10.1016/j.icesjms.2005.05.017>
- 832 Vollset, K.W., Catalán, I.A., Fiksen, Folkvord, A., 2013. Effect of food deprivation on  
833 distribution of larval and early juvenile cod in experimental vertical temperature  
834 and light gradients. Mar. Ecol. Prog. Ser. 475, 191–201.  
835 <https://doi.org/10.3354/meps10129>

## HIGHLIGHTS

USING SELF ORGANIZING MAPS TO ANALYZE LARVAL FISH ASSEMBLAGE

VERTICAL DYNAMICS THROUGH ENVIRONMENTAL-ONTOGENETIC GRADIENTS.

Álvarez, I<sup>1\*</sup>; Font-Muñoz, J S<sup>1,3</sup>; Hernández-Carrasco, I<sup>1</sup>; Díaz-Gil, C<sup>1,2</sup>; Salgado-Hernanz, P. M.<sup>1</sup>; Catalán, I. A.<sup>1</sup>

- Larval fish assemblages analysis with Self Organizing Maps allows overcoming linear constraints
- Self Organizing Maps analysis allowed the description of the whole coastal multispecific system
- Self Organizing Maps also allowed identifying ontogenetic differences in vertical positions
- Differences in larval fish vertical strategies before & after the establishment of stratification

**YECSS-D-20-00384 Author statement**

All the authors in the list have agreed to be listed and have approved the submitted version of the manuscript. I. Alvarez and I.A. Catalán proposed the research hypothesis, analyzed the larval fish assemblages, wrote and edited the manuscript. JS Font-Muñoz and I Hernández-Carrasco did the statistical analyses and actively participated in the writing of the MS. Finally, PM Salgado-Hernanz and C Diaz-Gil participated in all the surveys and in the manuscript writing.

Journal Pre-proof

**Declaration of interests**

The authors declare that they have no known competing financial interests or personal relationships that could have appeared to influence the work reported in this paper.

The authors declare the following financial interests/personal relationships which may be considered as potential competing interests:

Journal Pre-proof